

Scientific Report No. 1  
Contract N00140-68-C-0109  
May 1968



• a p p l i e d • m a t h e m a t i c s •

Transient Analysis of Transducer Arrays

by

Charles H. Sherman  
Dorothy A. Moran

This document is available  
for public release and its  
distribution is unlimited

for

U.S. Navy Underwater Sound Laboratory

R  
JUN 20 1968

**PARKE MATHEMATICAL LABORATORIES, Inc.**  
**One River Road • Carlisle, Massachusetts**

Reproduced by the  
CLEARINGHOUSE  
for Federal Scientific & Technical  
Information Springfield Va 22151

AD 670804

• P M I •

• P M I •

Scientific Report No. 1  
Contract N00140-68-C-0109  
May 1968



• a p p l i e d • m a t h e m a t i c s • •

• a p p l i e d • m a t h e m a t i c s •

Transient Analysis of Transducer Arrays

by

Charles H. Sherman  
Dorothy A. Moran

for

U.S. Navy Underwater Sound Laboratory

**PARKE MATHEMATICAL LABORATORIES, Inc.**  
**One River Road • Carlisle, Massachusetts**

### Abstract

A method for analyzing the transient behaviour of the transducer velocities in an array of transducers is described and used to obtain results for several typical situations. The method is based on a finite difference iteration solution of the differential equations for the array. It uses results of Mangulis for the transient self acoustic loading and makes approximations for the acoustic interactions based on Rayleigh's general expression for the field of a source in an infinite, rigid plane. The results obtained are for small plane arrays of small circular pistons. They show that the transient period can be considerably extended by the interactions and that effects of practical importance such as velocity overshoots often occur during the transient period.

Table of Contents

Introduction . . . . .	1
Formulation of the Problem . . . . .	2
The Numerical Method . . . . .	8
Results. . . . .	11
Conclusion . . . . .	17
Acknowledgement. . . . .	17
References . . . . .	36

**BLANK PAGE**

## Introduction

The use of large transducer arrays in Sonar has stimulated interest in transient effects, because the interactions between transducers modify the familiar transient behaviour of isolated transducers. The transient period of each transducer is extended as the delayed interactions from other distant transducers gradually exert their influence. The transient behaviour of each transducer also depends on its location in the array since the interactions enter in a different order at each location. Finally, some of the more drastic interaction effects, resulting in mechanical or electrical damage, might occur during the transient period and be unpredictable by steady state analysis.

We have studied various methods for analyzing the transient behaviour of transducer arrays<sup>1,2</sup> and now present a detailed description of one of these methods with examples of results which have been obtained. For simplicity the method will be presented in terms of a specific transducer equivalent circuit, but it could be applied to other cases. In the method to be described here the transient interactions are treated in an approximate manner. These approximations can be improved by use of other methods.<sup>2</sup>

In the present work the emphasis is on the transient build-up of the transducer velocities. In earlier work<sup>3</sup> we studied the build-up of the near field sound pressure at certain points on the surface of simple

arrays assuming that the velocity was specified. The next step should be the use of transient velocity results such as those to be reported here as the basis for transient near field pressure calculations.

Formulation of the Problem

We will assume that the usual lumped electromechanical equivalent circuits are adequate for use under transient conditions. For a piezoceramic transducer with a parallel tuning coil and neglecting electrical losses we have the circuit shown in Fig. 1 where the circuit elements have their standard meanings.  $e_j$  is the applied voltage,  $v_j$

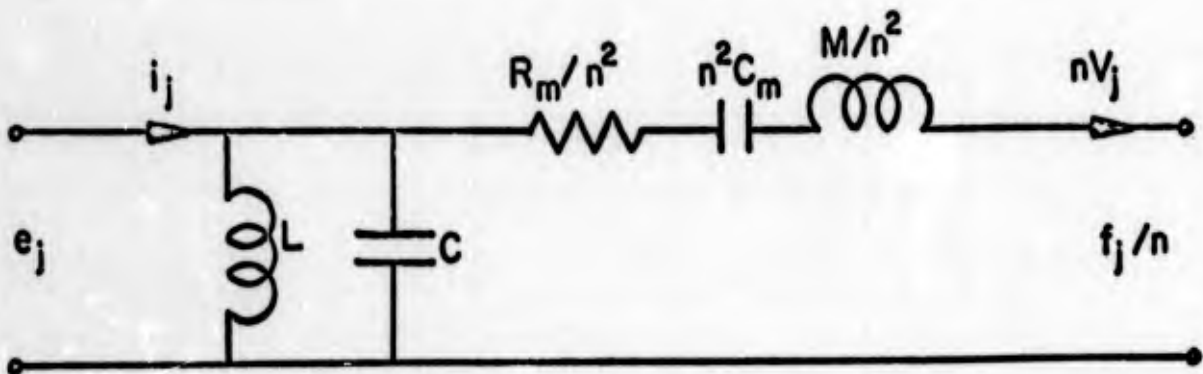


Fig. 1. Transducer equivalent circuit used to describe the method and for the numerical examples.

is the transducer velocity, and  $f_j$  is the force exerted by the sound field on the radiating face of the transducer which includes all the interaction forces. These variables are related by

$$n e_j = M \frac{d v_j}{dt} + R_m v_j + \frac{1}{C_m} \int_0^t v_j dt' + f_j, \quad (1)$$

$$j = 1, 2, \dots, N,$$

where we are considering an array of  $N$  identical transducers.

If there were no acoustic forces ( $f_j = 0$ ) we would have a simple transient problem with familiar results. For an isolated transducer in a medium where  $f_j$  only involves the self radiation force the general form of these familiar results would not be strongly modified for transducers of the usual sizes where the propagation time across the transducer was only a fraction of a period of the driving frequency. This point will be illustrated later. But for a large array of transducers where  $f_j$  includes the interaction forces the results can be considerably modified as we shall see.

For an array of  $N$  transducers, assuming linear acoustics, we can write the total acoustic force as

$$f_j = \sum_{i=1}^N \int_{S_i} p_i dS_i, \quad (2)$$

where  $p_i$  is the pressure produced by the  $i^{\text{th}}$  transducer, and the integration extends over the surface of the  $j^{\text{th}}$  transducer. For vibrating surfaces in an infinite, rigid plane we can use Rayleigh's expression for the velocity potential<sup>4</sup> and obtain for  $p_i$ ,

$$p_i = \frac{\rho}{2\pi} \frac{\partial}{\partial t} \int_{S_i} \frac{i}{r_{ij}} v_i (t - r_{ij}/c) dS_i, \quad (3)$$

where  $r_{ij}$  is the distance from the area element  $dS_i$  on the  $i^{\text{th}}$  transducer surface to a point on the  $j^{\text{th}}$  surface,  $\rho$  is the density of the medium and  $c$  is the speed of sound. Since it is difficult to use Eq. (3) as it is, we will make simplifying approximations and treat the self and interaction forces differently.

We will confine ourselves to transducers with circular radiating faces and use the work of Mangulis<sup>5</sup> for the self radiation forces. He solved the problem of the transient loading of a circular piston when a sinusoidal velocity is suddenly applied. In our problem we will assume that a sinusoidal voltage is suddenly applied at the electrical terminals of the transducer, and thus we will not have an abrupt sinusoidal velocity. However, we can reasonably expect that the velocities will be approximately sinusoidal with time varying amplitudes which do not change drastically in one period of the driving voltage. Under such conditions Mangulis' results should be a good approximation. We can write the self radiation force in the form

$$f_{jj}(t) = R_{jj}(t) v_j + \frac{1}{\omega} X_{jj}(t) \frac{dv_j}{dt} \quad (4)$$

where  $\omega$  is the angular frequency of the sinusoidal driving voltage.

$R_{jj}(t)$  and  $X_{jj}(t)$  are the time dependent self radiation resistance and reactance given by Mangulis as

$$\frac{R_{jj}(T)}{\rho c A} = \begin{cases} 1 - \frac{4}{\pi} \int_{\cos^{-1} T/2ka}^{\pi/2} \sin^2 \theta \cos(2ka \cos \theta) d\theta, & 0 \leq T \leq 2ka \\ 1 - \frac{J_1(2ka)}{ka}, & T \geq 2ka \end{cases} \quad (5)$$

$$\frac{X_{jj}(T)}{\rho c A} = \begin{cases} \frac{4}{\pi} \int_{\cos^{-1} T/2ka}^{\pi/2} \sin^2 \theta \sin(2ka \cos \theta) d\theta, & 0 \leq T \leq 2ka \\ \frac{S_1(2ka)}{ka}, & T \geq 2ka \end{cases} \quad (6)$$

In these equations we have used the variable  $T = \omega t$ ;  $A$  is the area of the circular piston,  $a$  is its radius and  $J_1$  and  $S_1$  are first order Bessel and Struve functions. The resistance ratio varies from unity at  $T = 0$  to its steady state value at  $T = 2ka$ , while the reactance ratio varies from zero at  $T = 0$  to its steady state value at  $T = 2ka$ . Thus the acoustic transient effects connected with the self radiation force end at  $T = 2ka$  which for typical transducer sizes is about half the period of the applied sinusoidal voltage.

We will approximate the transient interaction forces by using step functions to give the propagation delay from the center of one transducer to the center of the other. This approximation includes the essential feature of the transient interaction, but it ignores the details of the build-up from zero to the steady state value. It is a reasonable approximation for small transducers, since the build-up time in radians is  $2ka$ . For small identical transducers we can approximate Eq. (3) in an obvious way and write

$$f_{ij} = \int_{S_j} p_i dS_j \approx \frac{\rho A^2}{2\pi d_{ij}} \frac{d}{dt} [v_i(t - d_{ij}/c)] S(t - d_{ij}/c) \quad (7)$$

where  $d_{ij}$  is the distance between the centers of the  $i^{\text{th}}$  and  $j^{\text{th}}$  transducers, and

$$S(t - d_{ij}/c) = \begin{cases} 0, & t < d_{ij}/c \\ i, & t \geq d_{ij}/c \end{cases}$$

The significance of Eq. (7) can be seen more clearly by considering a time  $t \gg d_{ij}/c$  when the steady state has been reached and the

velocity can be written in complex form as

$$v_i(t) = V_i e^{i\omega t}$$

Then with  $A = \pi a^2$  we have

$$f_{ij} = \left[ \rho c A \frac{1}{2} (ka)^2 \frac{ie^{-ikd_{ij}}}{kd_{ij}} \right] V_i e^{i\omega t}$$

and the expression in brackets is a well known approximation for the mutual radiation impedance between small circular pistons.<sup>6</sup> Thus Eq. (7) approaches the correct values for small transducers as the steady state is approached.

Using these expressions for the radiation forces, and specifying the applied voltage as

$$e_j = \begin{cases} 0, & T < 0 \\ E_j \cos(T + \delta_j), & T \geq 0 \end{cases} \quad (8)$$

we can now rewrite Eq. (1) for  $T \geq 0$ :  $j = 1, 2, \dots, N$

$$\begin{aligned} nE_j \cos(T + \delta_j) = & [\omega M + X_{jj}(T)] \frac{dv_j}{dT} + [R_m + R_{jj}(T)] v_j \\ & + \frac{1}{\omega C_m} \int_0^T v_j(T') dT' \\ & + \frac{1}{2} \rho c A (ka)^2 \sum_{l \neq j} \frac{1}{kd_{lj}} \frac{d}{dT} [v_l(T - kd_{lj})] S(T - kd_{lj}). \end{aligned} \quad (9)$$

This is the set of equations which must be solved to determine all the transducer velocities as a function of time. These equations are uncoupled in the beginning, from  $T=0$  to  $T = (kd_{ij})_{\text{minimum}}$ . Then propagation of sound brings the first interactions into effect. As more and more interactions enter the picture the equations gradually

become more strongly coupled until when  $T = (kd_{ij})_{\text{maximum}}$  each equation is coupled to every other equation.

The applied voltage specified in Eq. (8) corresponds to simultaneous application of all the voltages with arbitrary phase relations and approximates the use of phase shifting networks for beam steering. The use of delay lines would correspond to applying the voltages at different times. The differences resulting from these two methods of phasing during the transient period were studied to some extent in earlier work.<sup>3</sup>

During the time period from  $T = 2ka$  to  $T = (kd_{ij})_{\text{minimum}}$  Eq. (9) has the simplest form, because the self radiation resistance and reactance have reached their constant steady state values and the interactions have not yet started. It is convenient to introduce the customary transducer parameters in terms of the coefficients in the equation in this form. Thus we write

$$\omega M + X_{ij}(\omega) = \frac{\omega}{\omega_0} \frac{g}{\kappa} R_{ij}(\omega), \quad (10)$$

$$R_m + R_{ij}(\omega) = \frac{1}{\kappa} R_{ij}(\omega), \quad (11)$$

$$1/\omega C_m = \omega_0/\omega \frac{g}{\eta} R_{ij}(\omega), \quad (12)$$

where

$$R_{ij}(\omega) = g c A [1 - J_1(2ka)/ka], \quad (13)$$

$$X_{ij}(\omega) = \rho c A S_1(2ka) / k_a \quad (14)$$

Solving Eqs. (10)-(12) for  $\eta$ ,  $Q$  and  $\omega_0$  shows that  $\eta$  is the mechano-acoustical efficiency,  $Q$  is the quality factor, and  $\omega_0$  is the angular resonant frequency for an isolated transducer under steady state conditions.

During the time period from  $T=0$  to  $T=2ka$  when the first two coefficients in Eq. (9) vary with time we can use Eqs. (10) and (11) to make the substitutions

$$\omega M = \frac{\omega}{\omega_0} \frac{Q}{\eta} R_{ij}(\omega) - X_{ij}(\omega), \quad (15)$$

$$R_m = R_{ij}(\omega) \left( \frac{1}{\eta} - 1 \right). \quad (16)$$

Thus we express the mass, internal resistance and compliance of the transducers in terms of the parameters  $Q$ ,  $\eta$ ,  $\omega_0/\omega$  and  $ka$ . Since the mass  $M$  is positive the possible sets of parameters are restricted by Eq. (15). It is necessary to have

$$\omega/\omega_0 \frac{Q}{\eta} \left[ 1 - \frac{J_1(2ka)}{ka} \right] > \frac{S_1(2ka)}{k_2}.$$

#### The Numerical Method

In the next step we approximate the derivatives in Eq. (9) by finite differences as follows:

$$\frac{dN}{dT} = \frac{1}{\Delta T} [N(T+\Delta T) - N(T)].$$

In Mangulis' results in Eqs. (5) and (6) we change the integration variable to  $x = \cos \theta$  which simplifies the integrals somewhat. We also define the quantity

$$F_j = n E_j / \rho c A.$$

Now we combine all the foregoing results and write out Eq. (9) for the three time regions:

$$\begin{aligned} & \underline{0 \leq T \leq 2ka} \\ F_j \cos(T + \delta_j) = & \left\{ \frac{\omega}{\omega_0} \frac{Q}{\eta} \left[ 1 - \frac{J_1(2ka)}{ka} \right] - \frac{S_1(2ka)}{ka} + \frac{4}{\pi} \int_0^{1/2ka} (1-x^2)^{1/2} \sin(2kax) dx \right\} \left[ \frac{N_j(T+\Delta T) - N_j(T)}{\Delta T} \right] \\ & + \left\{ \left( \frac{1}{\eta} - 1 \right) \left[ 1 - \frac{J_1(2ka)}{ka} \right] + 1 - \frac{4}{\pi} \int_0^{1/2ka} (1-x^2)^{1/2} \cos(2kax) dx \right\} N_j(T) \\ & + \frac{\omega_0}{\omega} \frac{Q}{\eta} \left[ 1 - \frac{J_1(2ka)}{ka} \right] \int_0^T N_j(T') dT' \end{aligned} \quad (17a)$$

$$\begin{aligned} & \underline{2ka \leq T \leq (kd_{ij})_{\text{minimum}}} \\ F_j \cos(T + \delta_j) = & \left[ 1 - \frac{J_1(2ka)}{ka} \right] \left\{ \frac{\omega}{\omega_0} \frac{Q}{\eta} \left[ \frac{N_j(T+\Delta T) - N_j(T)}{\Delta T} \right] + \frac{1}{\eta} N_j(T) \right. \\ & \left. + \frac{\omega_0}{\omega} \frac{Q}{\eta} \int_0^T N_j(T') dT' \right\} \end{aligned} \quad (17b)$$

$$\begin{aligned} & \underline{T \geq (kd_{ij})_{\text{minimum}}} \\ F_j \cos(T + \delta_j) = & \left[ 1 - \frac{J_1(2ka)}{ka} \right] \left\{ \frac{\omega}{\omega_0} \frac{Q}{\eta} \left[ \frac{N_j(T+\Delta T) - N_j(T)}{\Delta T} \right] + \frac{1}{\eta} N_j(T) + \frac{\omega_0}{\omega} \frac{Q}{\eta} \int_0^T N_j(T') dT' \right. \\ & \left. + \sum_{i \neq j} \frac{1}{kd_{ij}} \left[ \frac{N_i(T+\Delta T - kd_{ij}) - N_i(T - kd_{ij})}{\Delta T} \right] S(T - kd_{ij}) \right\} \end{aligned} \quad (17c)$$

In Eq. (17c) the factor  $\frac{1}{2}(ka)^2$  was replaced by  $[1 - J_1(2ka)/ka]$  which is more consistent with the self radiation force and has about the same value for  $ka \leq \frac{1}{2}$ .

Eqs. (17a)-(17c) were programmed for the IBM 1130 computer to obtain the velocity of each transducer as a function of time starting with initial conditions of zero velocity. Note that it was implied in Eq. (1) that the initial displacements were zero. It was found that the time increment  $\Delta T$  could not exceed about .02 radians for reasonable accuracy. Thus about 300 steps per cycle of the driving voltage were required. One program was written specifically for line arrays where all the  $kd_{ij}$  are integral multiples of  $(kd_{ij})_{\text{minimum}}$ . Then by making  $(kd_{ij})_{\text{minimum}}$  an integral multiple of  $\Delta T$  the computations could be carried out without interpolation between previously calculated values. Another program was written for arbitrary locations of the transducers in a plane for which interpolation was required.

The accuracy of the numerical computations as well as the adequacy of the various approximations was tested by computing the velocities until steady state was approximately attained and then comparing the velocity amplitudes with those obtained from independent steady state calculations. The steady state calculations were done by D.T. Porter at USNUSL. Agreement to within a few per cent was found as long as  $\Delta T$  did not exceed .02 radians. Table 1 compares the results for the case of a ten element line array driven with the same amplitudes ( $F_j = 1$ ) and phases ( $\delta_j = 0$ ) using  $ka = .5$ ,  $\eta = .5$ ,  $\omega = \omega_0$ ,  $Q = 2$  and quarter

wavelength separation between adjacent transducers (transducer number one is on the end). The computations were continued for about nine cycles, and it appeared that the steady state amplitudes had been reached to within less than 1%. The low  $Q$  hastens the approach to

Table 1. Comparison of transient calculations with independent steady state calculations

<u>Transducer</u>	<u>Steady State Velocity Amplitude</u>	
	<u>from transient</u>	<u>from steady state</u>
1	3.57	.48
2	2.32	2.31
3	2.79	2.72
4	3.19	3.11
5	2.56	2.52

steady state, but in this case, where the array is 2.25 wavelengths long, the interactions still cause minor transient fluctuations for several cycles. The differences in Table 1 are probably caused mainly by our approximation of the interactions, which requires  $\lambda a < .5$ .

### Results

In Fig. 2 we show the effect on the transducer velocity of using Mangulis' transient radiation impedance as compared to using the steady state radiation impedance. The difference between the velocities is small at first and gradually disappears after  $T = 2\lambda a$ , showing that acoustic transient effects do not change the transient behaviour of small isolated transducers very much. As can be seen from the lower

part of the figure the transient radiation resistance is very high in the beginning. This makes the velocity nearly in phase with the driving voltage so that it approaches its steady state amplitude more quickly. Thus the transient radiation impedance makes the velocity attain a higher value at its first peak as shown. In other words the transient radiation impedance makes the transducer behave as though it had a very low  $Q$  at the beginning.

Note that  $F = \frac{ne}{\epsilon c A}$  has the units of velocity. The velocity values in Fig. 2 and subsequent results calculated for  $F = 1$  are then in units of  $\frac{ne}{\epsilon c A}$ .

Figures 3 and 4 show the velocities as a function of time for a 3 by 1 array. The  $ka$  of the circular pistons is 0.5. The efficiency of the transducers is 50%, the  $Q$  is 4 and the driving frequency equals the resonant frequency. These parameters refer, as given in Eqs. (10)-(12), to an isolated transducer. The interaction impedances modify the radiation resistance and reactance causing the actual efficiency,  $Q$  and resonant frequency to vary depending on location in the array. The separation between transducers is a quarter wavelength. The driving voltage amplitudes and phases are equal, and the voltage wave form in these figures is just cost.

The velocities of the two transducers on the ends of this 3 by 1 array build up to steady state in a way that is very similar to that for an isolated transducer. For example, after  $Q$  cycles the amplitude is within a few per cent of its final value. The velocity of the

transducer in the middle shows slightly more interesting behaviour. After about two cycles it builds up to a maximum and then decreases slightly toward its steady state value. The steady state velocities are given in the figures.

In Figures 5 and 6 we consider transducers with the same parameters in a  $3 \times 2$  array. Because of the symmetry there are still only two different velocities. The velocities of the corner transducers simply increase steadily to their final value which is slightly lower than that for the end transducers in the  $3 \times 1$  array, because of the different interactions. But the velocities of the middle transducers now show a definite overshoot after about one cycle. Note, however, that the maximum velocity attained by the middle transducers is less than the steady state velocity of the end transducers.

Next in Figures 7-9 we have a  $3 \times 3$  array of the same transducers. The corner velocities build up in about the same way as before. The side velocities build up very quickly with a slight overshoot. The velocity of the center transducer shows the most interesting behaviour. It starts to build up, but all the interactions from the other transducers which surround it soon load it heavily and cause it to decrease to a very small value before it starts to increase again. It apparently takes several more cycles to reach the steady state value of 0.76.

The total radiation impedance obtained from Porter's steady state calculations for the  $3 \times 3$  array are given in Table 2. The most notable feature of these results is the large negative radiation resistance of

the center element.

Table 2. Total radiation impedance and steady state velocity amplitude of the transducers in the 3 x 3 array with  $ka = 0.5$  used for Figures 7-9.

<u>Transducer</u>	<u><math>R/gcA</math></u>	<u><math>X/gcA</math></u>	<u>Steady state velocity amplitude</u>
corner	0.15	0.30	3.46
side	0.44	0.19	1.69
center	-1.43	0.31	0.76

Such absorption of energy from the sound field is common for a transducer in such a location relative to the other transducers. It can also be seen from Figures 7-9 that the velocities of the corner and side transducers are approximately in phase after 5-6 cycles, while the center transducer is almost  $180^\circ$  out of phase with the others.

Figure 9 shows that for the center transducer in the 3 x 3 array it takes considerable time for the interactions to have their full effect. The interactions from the four transducers on the sides of the array begin at  $T = 1.58$  radians, while those from the four corner transducers start at  $T = 2.23$  radians. However, these interactions are weak until the velocity of these outside transducers build up, and the effect on the center transducer doesn't become noticeable until  $T \approx 6$  radians. Then the impedance magnitude of the center transducer begins to increase and its velocity to decrease. Note that  $\eta = .5$  and  $R_{ii} \approx .12 gcA$  means that the internal resistance  $R_m \approx .12 gcA$ . The total resistance in the steady state is then  $(.12 - 1.43) gcA = -1.31 gcA$ , and the

center transducer has a greater impedance magnitude than the others.

Figures 10-19 show the velocities of the transducers in a  $10 \times 1$  line array phased to end fire with transducer parameters of  $\eta = 1$  and  $Q = 10$  chosen to emphasize both interaction effects and transient effects. The driving frequency is slightly below resonance ( $\omega/\omega_0 = 0.9$ ) which also gives more complicated transient effects. A definite pattern of velocity amplitude modulation appears in which the modulation frequency increases as we go toward the downstream end. This modulation frequency is approximately the difference between the driving frequency and the effective resonant frequency of the transducers in the array. The steady state calculations show that the total radiation reactance of the transducer on the downstream end is about  $.34 \rho c A$  which is slightly less than the self reactance of  $.397 \rho c A$ . This means that its effective resonant frequency is  $\sim 1.14\omega$ , and the difference frequency is  $1.14\omega - \omega = .14\omega$ , in agreement with the modulation frequency appearing in Fig. 19. There is an increase of radiation reactance along the array resulting in a decrease of resonant frequency and thus a decrease of modulation frequency. On the upstream end the total radiation reactance is  $\sim .58 \rho c A$ , the effective resonant frequency is  $\sim 1.04\omega$ , and the difference frequency is  $\sim .04\omega$ , which is similar to the modulation frequency in Fig. 10. Thus the modulation in Figures 10-19 comes from the mixing of the steady state and transient parts of the velocity.

This variation of radiation reactance and lowering of resonant

frequency along the array is also responsible for the variation of the steady state velocity amplitude from one transducer to the next. Thus the transducer on the upstream end is closer to resonance than any other, and it has the biggest velocity. However, transient effects are important here, because the velocity amplitude of this transducer reaches a value about 35% higher than its steady state value. Since this transducer has a higher steady state velocity than any other transducer in the array, we have a case where the damaging effects of high velocity could occur during the transient period.

The effects shown in Figures 10-19 are rather extreme because of the off-resonance operation with high  $Q$  and high efficiency, but they show the kind of situations which might be troublesome in practice. Calculations were also done for a 10 x 1 array of the same transducers in the broadside mode. Here too the transient velocity of the end transducer exceeded the highest steady state velocity. Probably the off-resonance driving is mainly responsible for this behaviour, but the extent to which it occurs is affected by the interactions and the phasing. A 10 x 1 array of transducers with  $Q=4$ ,  $\eta=.5$  and otherwise the same as those above was also tried at resonance and end fire. The velocity overshoots were small, and the transient effects did not persist beyond 5 or 6 cycles.

### Conclusion

We have not yet studied enough cases or sufficiently large arrays to permit firm general conclusions about the transient behaviour of practical Sonar arrays. However, it is clear that the transient period can be extended considerably by interaction effects and that velocity overshoots often occur. The calculations do suggest that the velocity attained in an overshoot at resonance does not exceed the steady state velocity of some other transducer in the array. In other words, overshoots only seem to occur at resonance for transducers which have relatively low steady state velocity. However, in cases such as the end fire array below resonance the transient velocities can exceed the steady state velocities. In such cases steady state analysis would not reveal situations which might cause transducer damage.

### Acknowledgement

The writers are grateful to David T. Porter of the U.S. Navy Underwater Sound Laboratory for his participation in this work and especially for providing the steady state array calculations. We are also grateful to Nan E. Gordon and John L. Butler for their assistance.

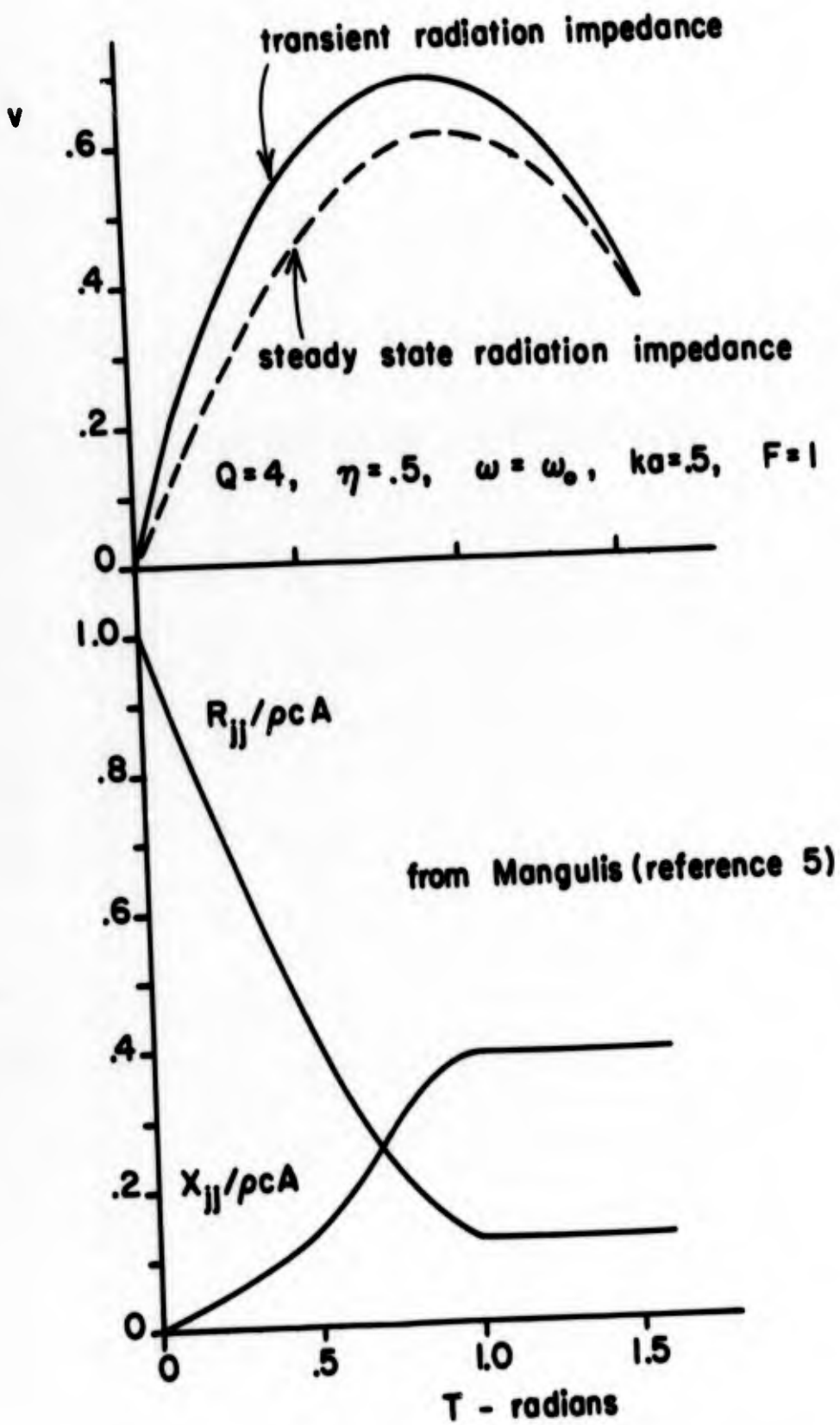


Fig. 2 Illustration of the effect on the velocity of using Mangulis' transient radiation impedance as compared to using the steady state radiation impedance.

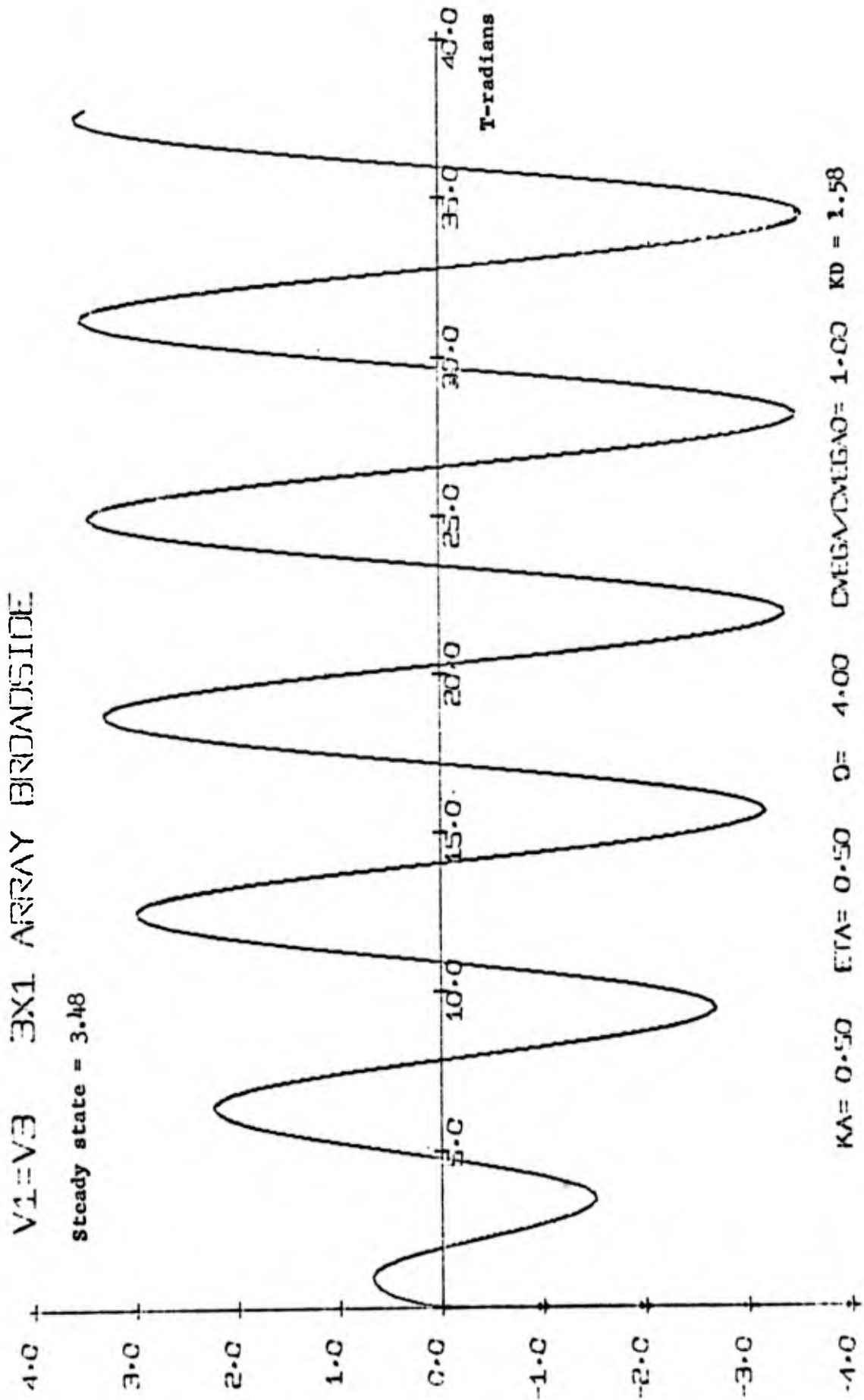


Fig. 3 Velocity of the end transducers in a 3 X 1 array driven with the same voltage amplitudes ( $F = 1$ ) in phase ( $\delta = 0$ ).

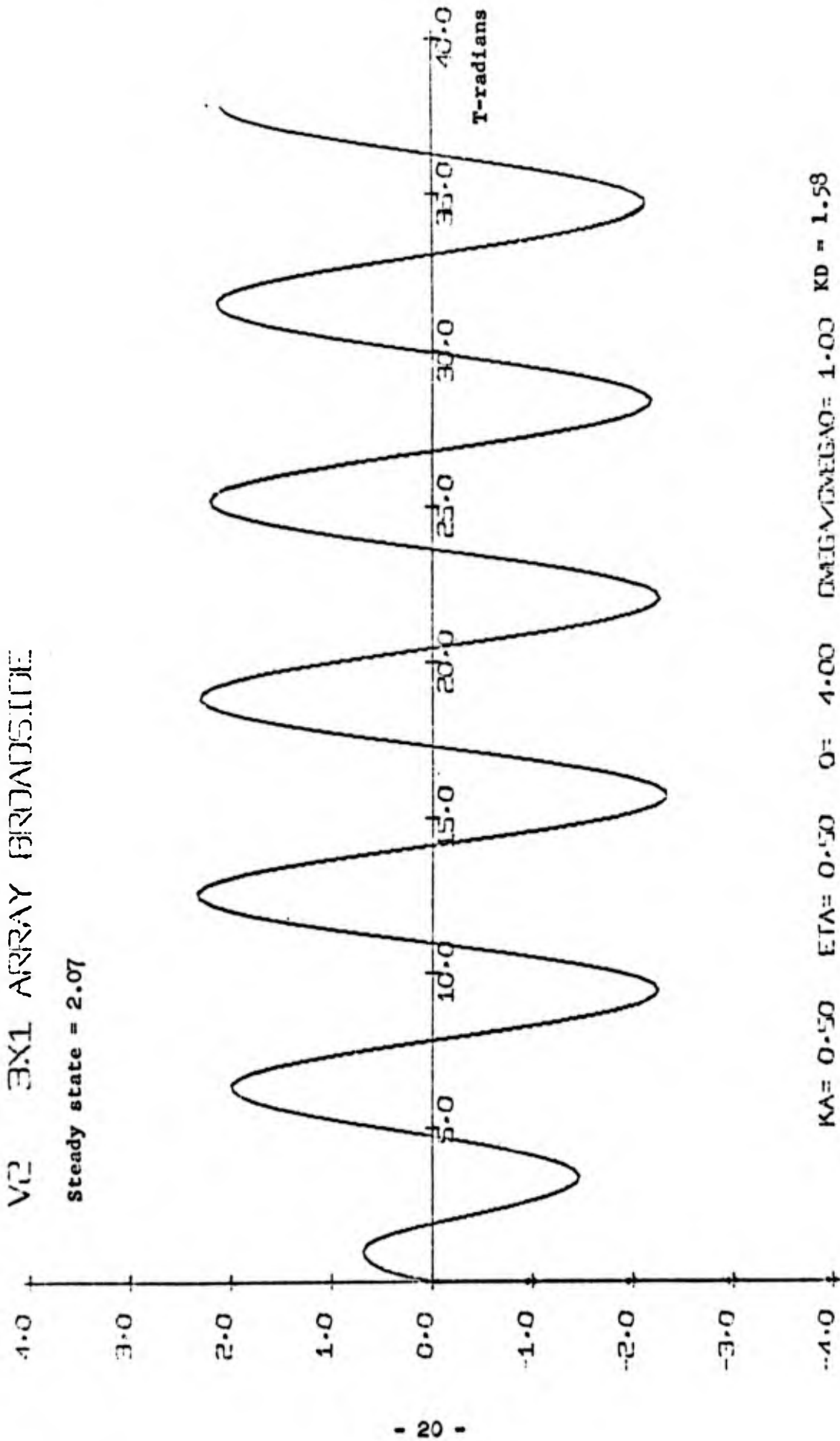
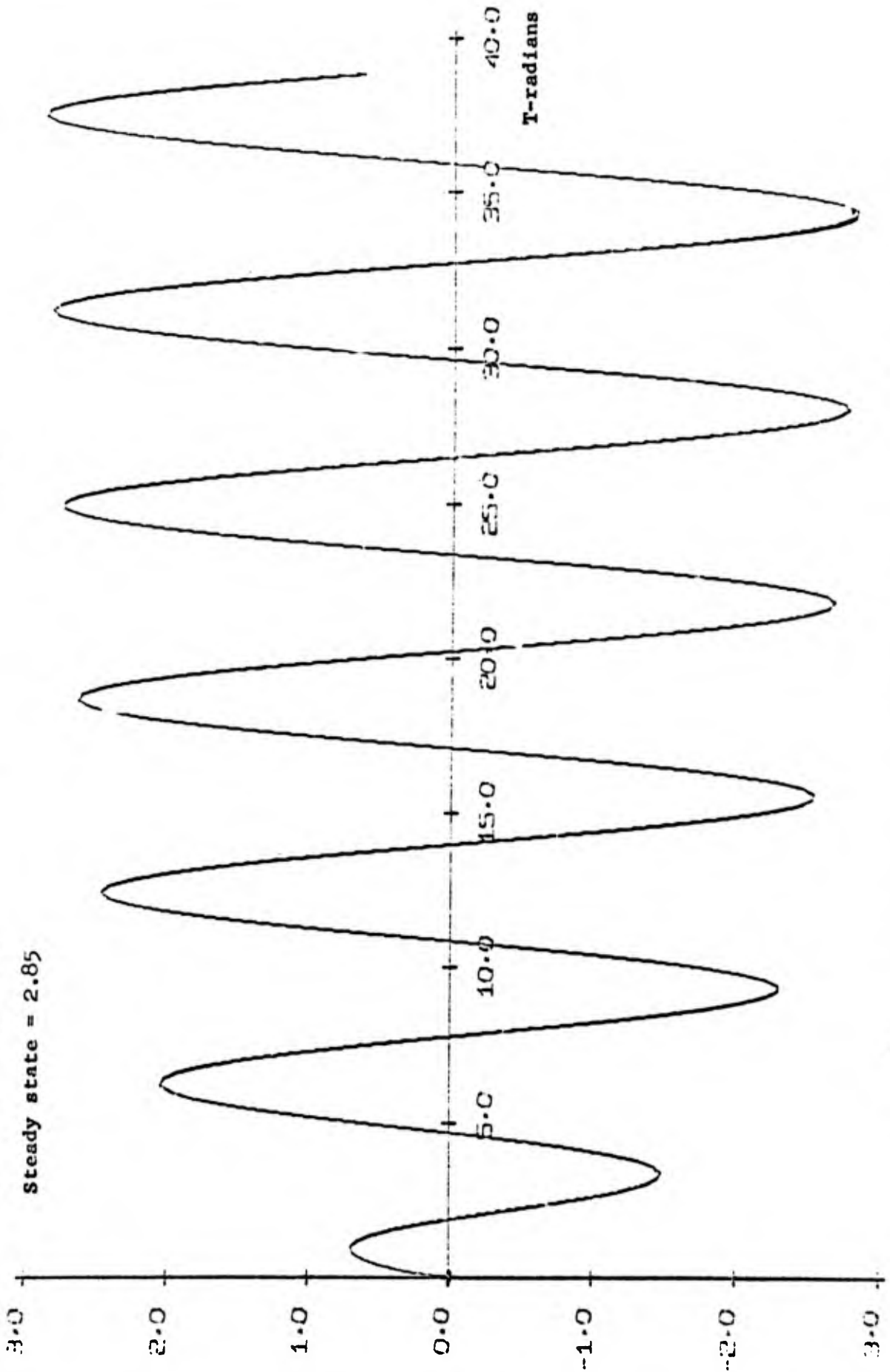


Fig. 4 Velocity of the middle transducer in a 3 X 1 array driven with the same voltage amplitudes ( $F = 1$ ) in phase ( $\delta = 0$ ).

V1 = V2 = V3 = V4    3X2 ARRAY BRUNALJUSTE

Steady state = 2.85

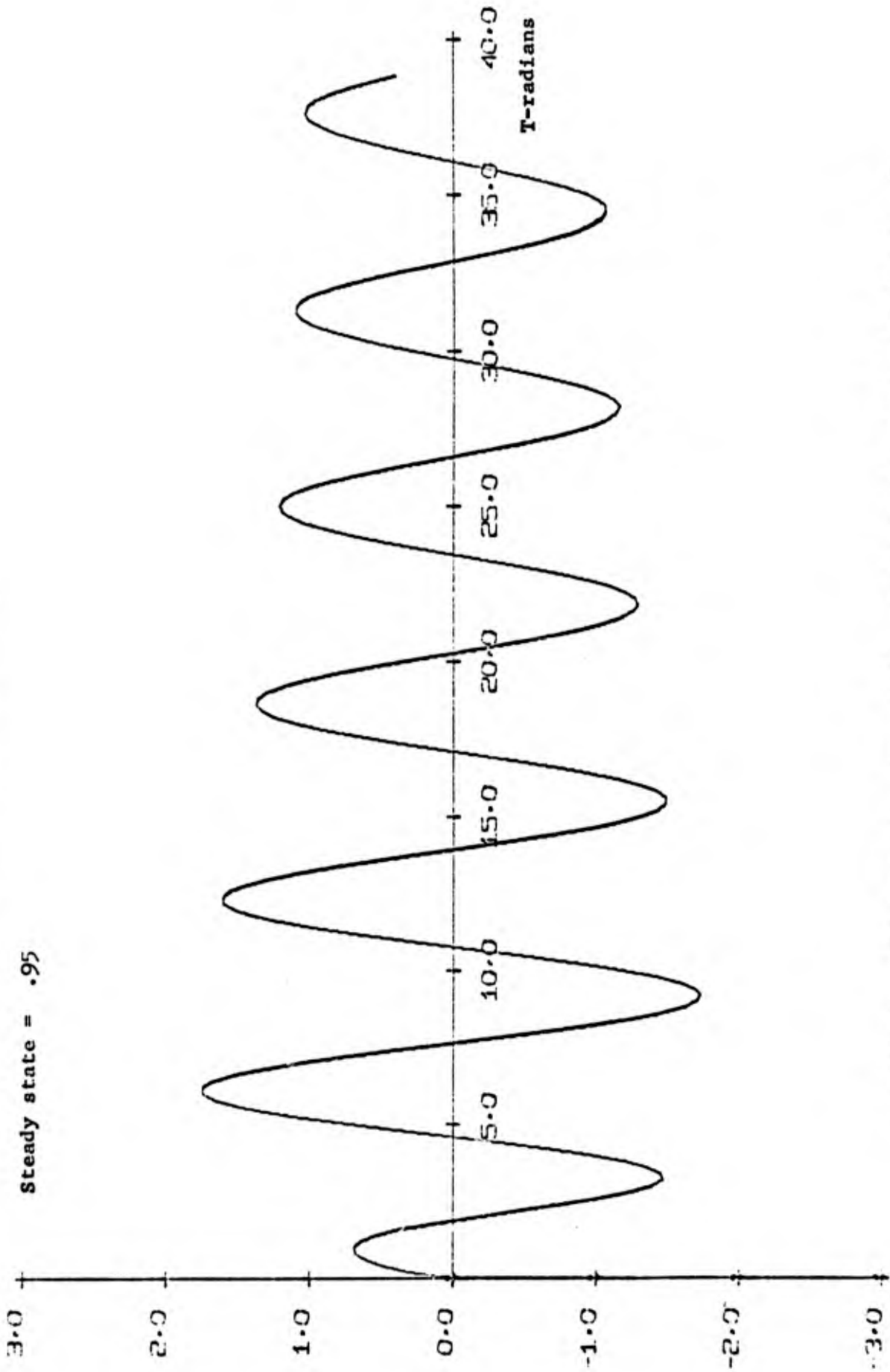


KA = 0.50    ETA = 0.50    Q = 1.00    ENFOA = ENFGAO = 1.00    KD = 1.58

Fig. 5 Velocity of the corner transducers in a 3 X 2 array driven with the

V<sub>3</sub> = V<sub>4</sub> 3X2 ARRAY BROADSIDE

Steady state = .95

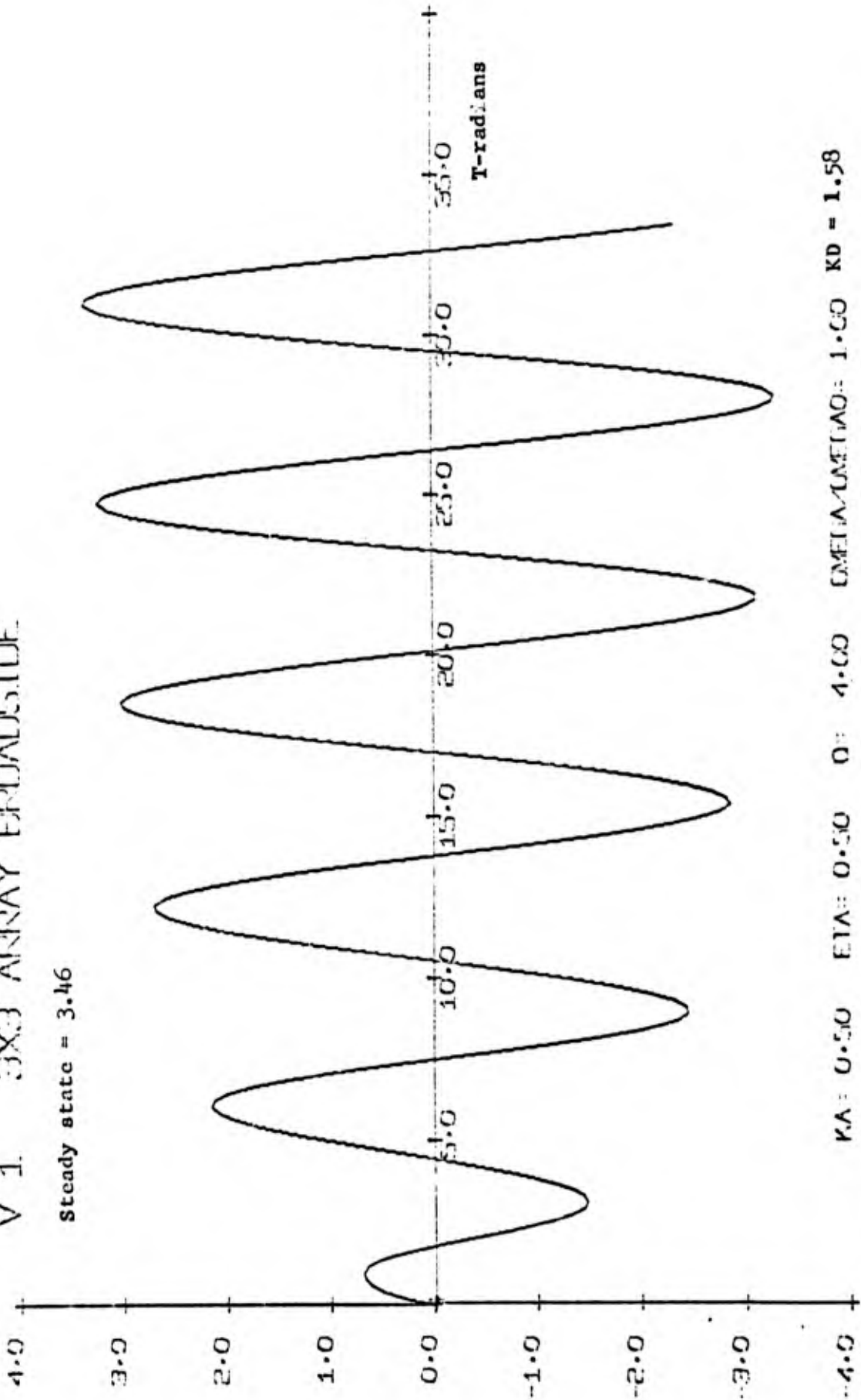


KA = 0.10    ETA = 0.50    Q = 4.00    LMEG/MEG<sub>0</sub> = 1.00    KD = 1.58

Fig. 6 Velocity of the middle transducers in a 3 X 2 array driven with the same voltage amplitudes ( $F = 1$ ) in phase ( $\delta = 0$ ).

V 1 3X3 ARRAY ENDALSIDE

Steady state = 3.46

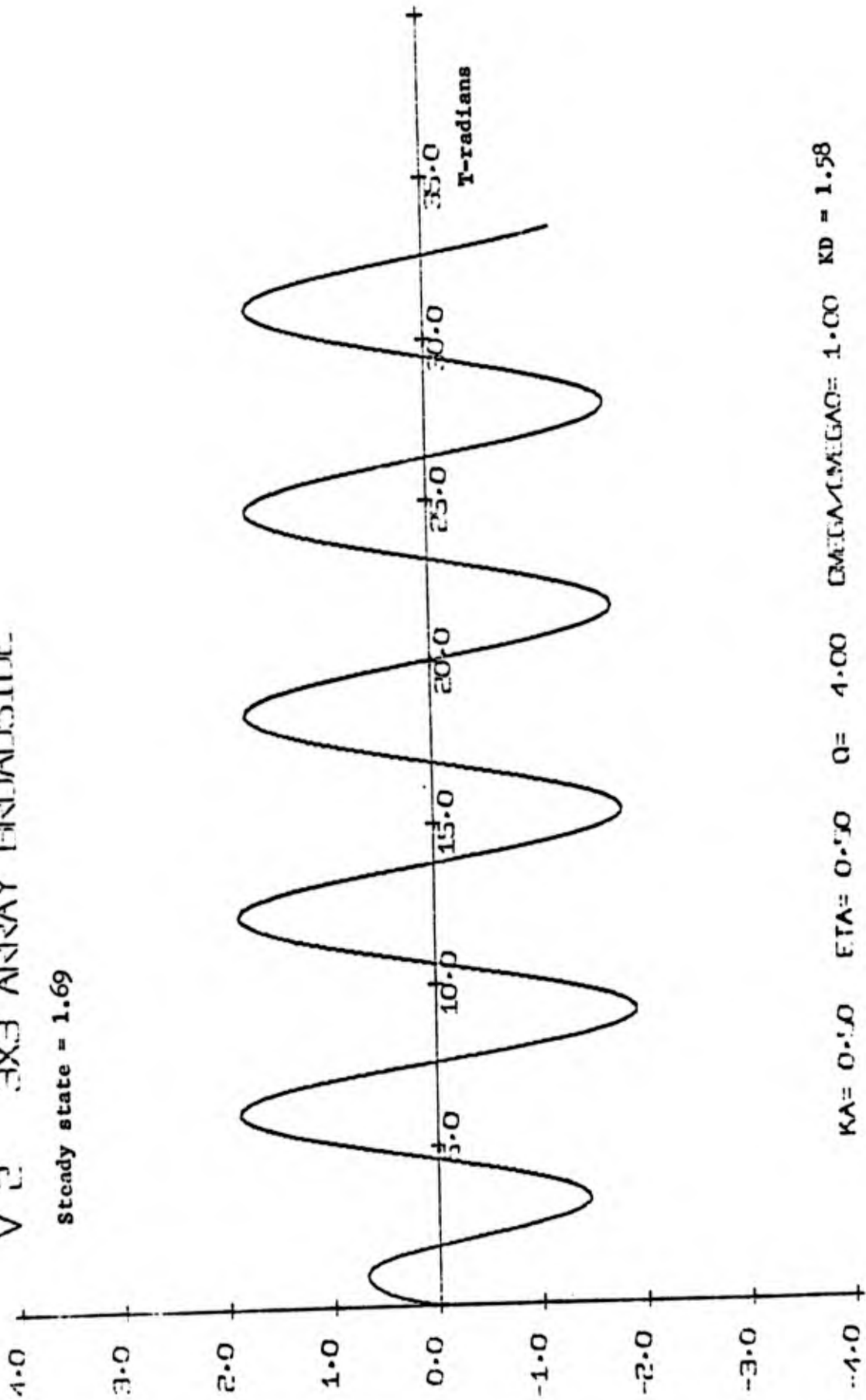


KA = 0.50 ETA = 0.50 Q = 4.00 DMEIA/DAE(TAO) = 1.00 KD = 1.58

Fig. 7 Velocity of the corner transducers in a 3 X 3 array driven with the same voltage amplitudes ( $F = 1$ ) in phase ( $\delta = 0$ ).

# V 2 3X3 ARRAY ENDSIDE

Steady state = 1.69



KA = 0.50    ETA = 0.50    Q = 4.00    CMEGAM (MEGAC) = 1.00    KD = 1.58

Fig. 8 Velocity of the side transducers in a 3 X 3 array driven with the same voltage amplitudes ( $V = 1$ ) in phase ( $\delta = 0$ ).

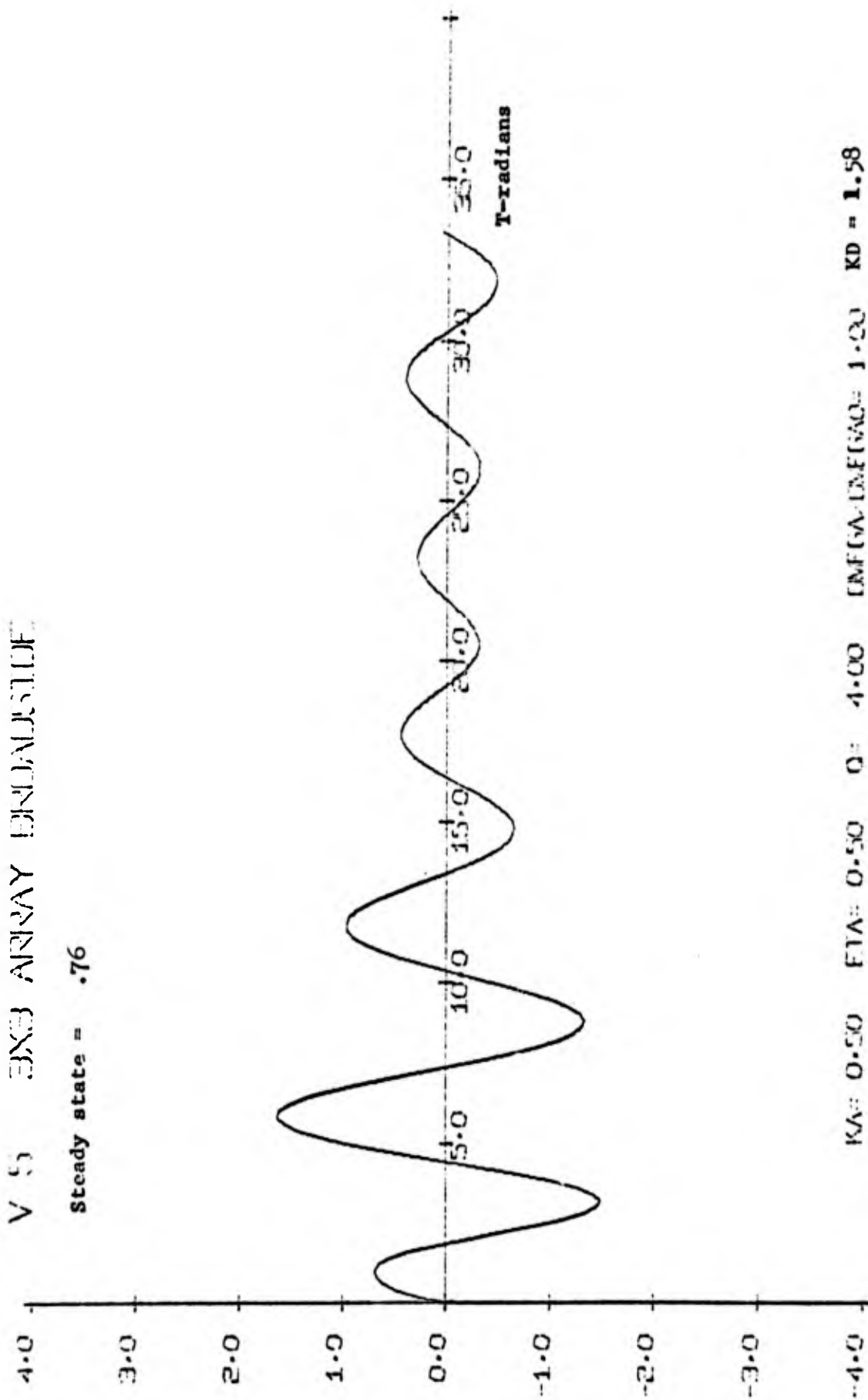


Fig. 9 Velocity of the center transducer in a 3 X 3 array driven with the same voltage amplitudes ( $F = 1$ ) in phase ( $\delta = 0$ ).

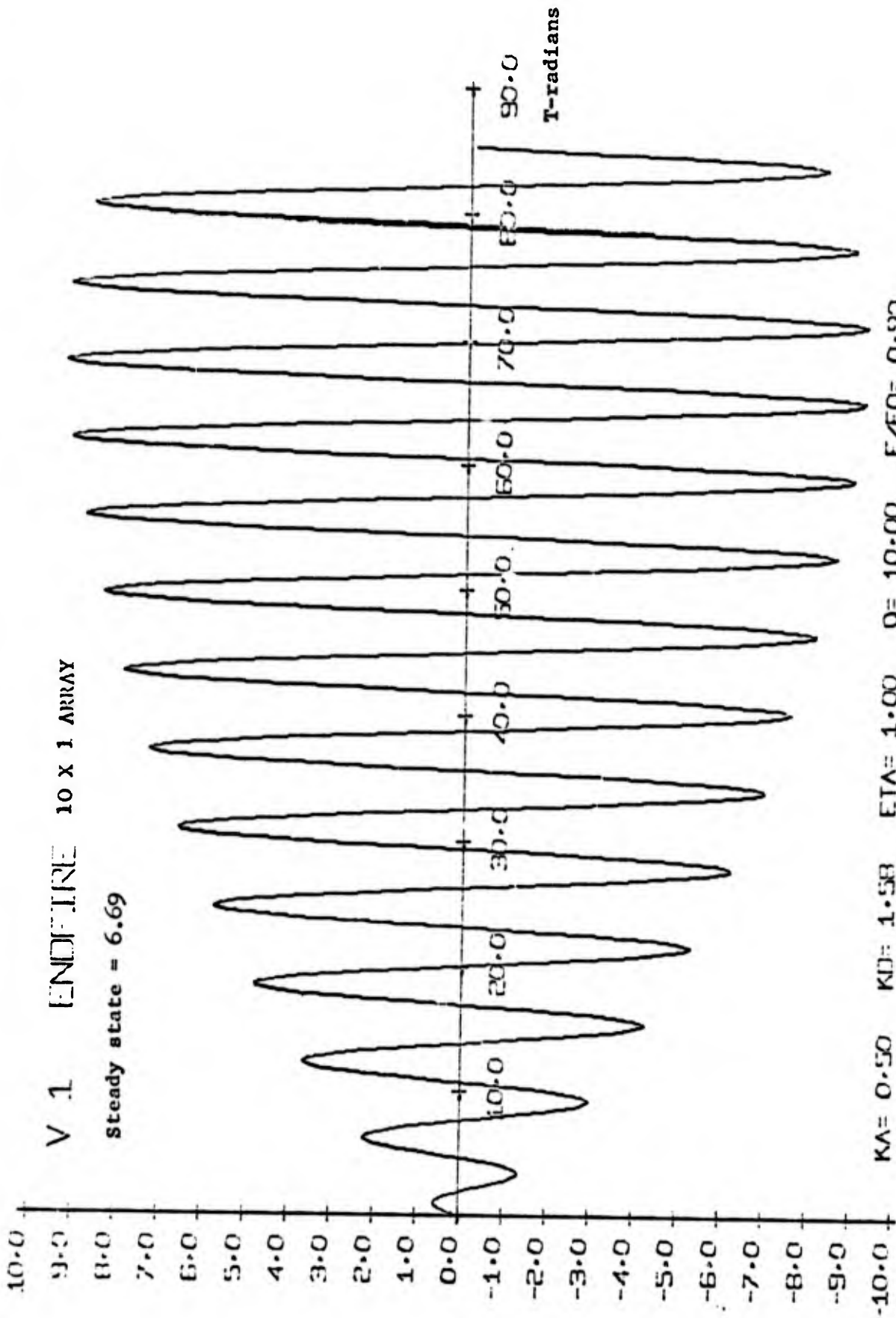


Fig. 10 Velocity of the transducer on the upstream end of a 10 X 1 line array phased to endfire ( $F = 1, \delta = 0$ ).

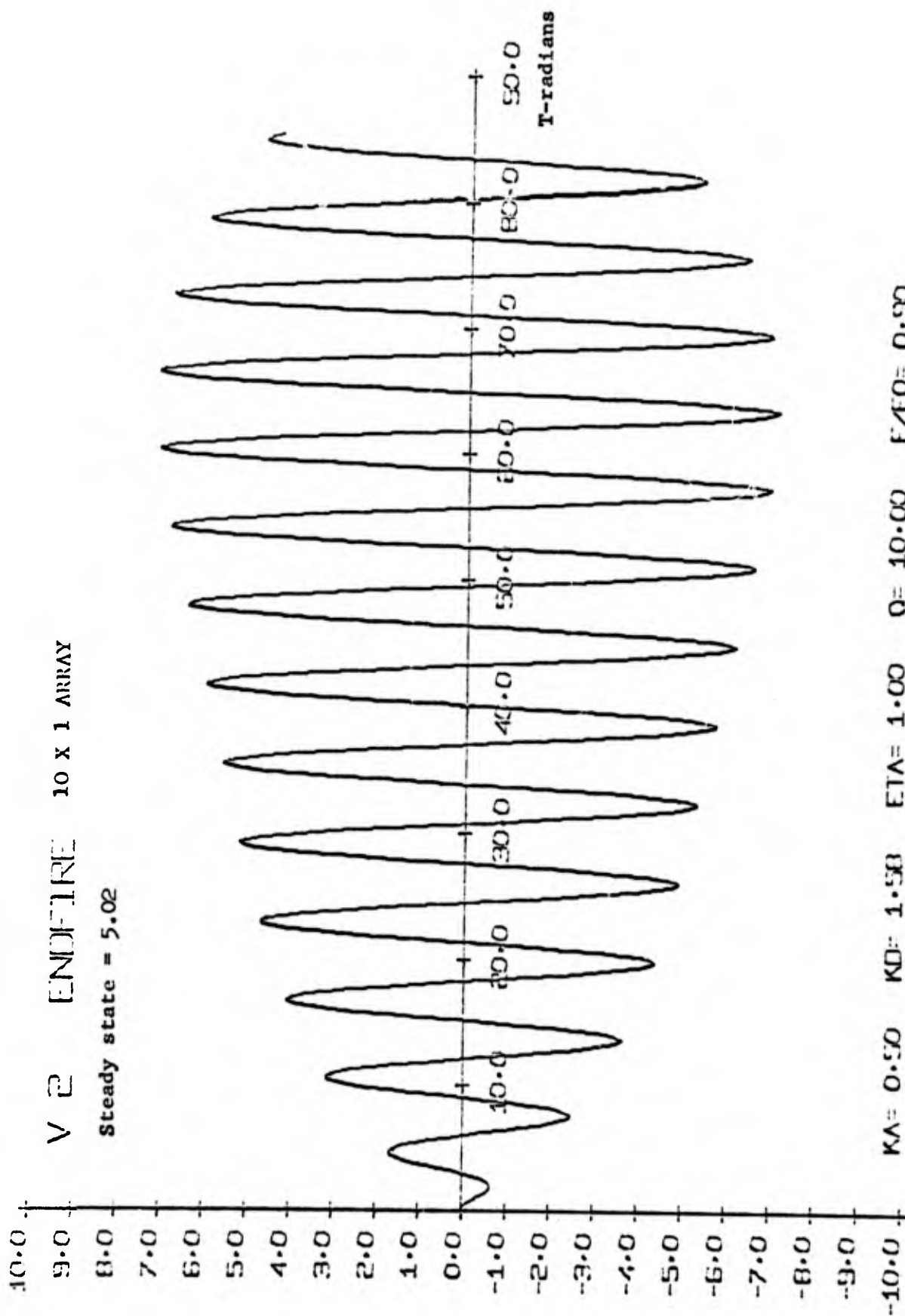


Fig. 11 Velocity of the second transducer in a 10 X 1 line array phased to endfire ( $F = 1, \delta = \pi/2$ ).

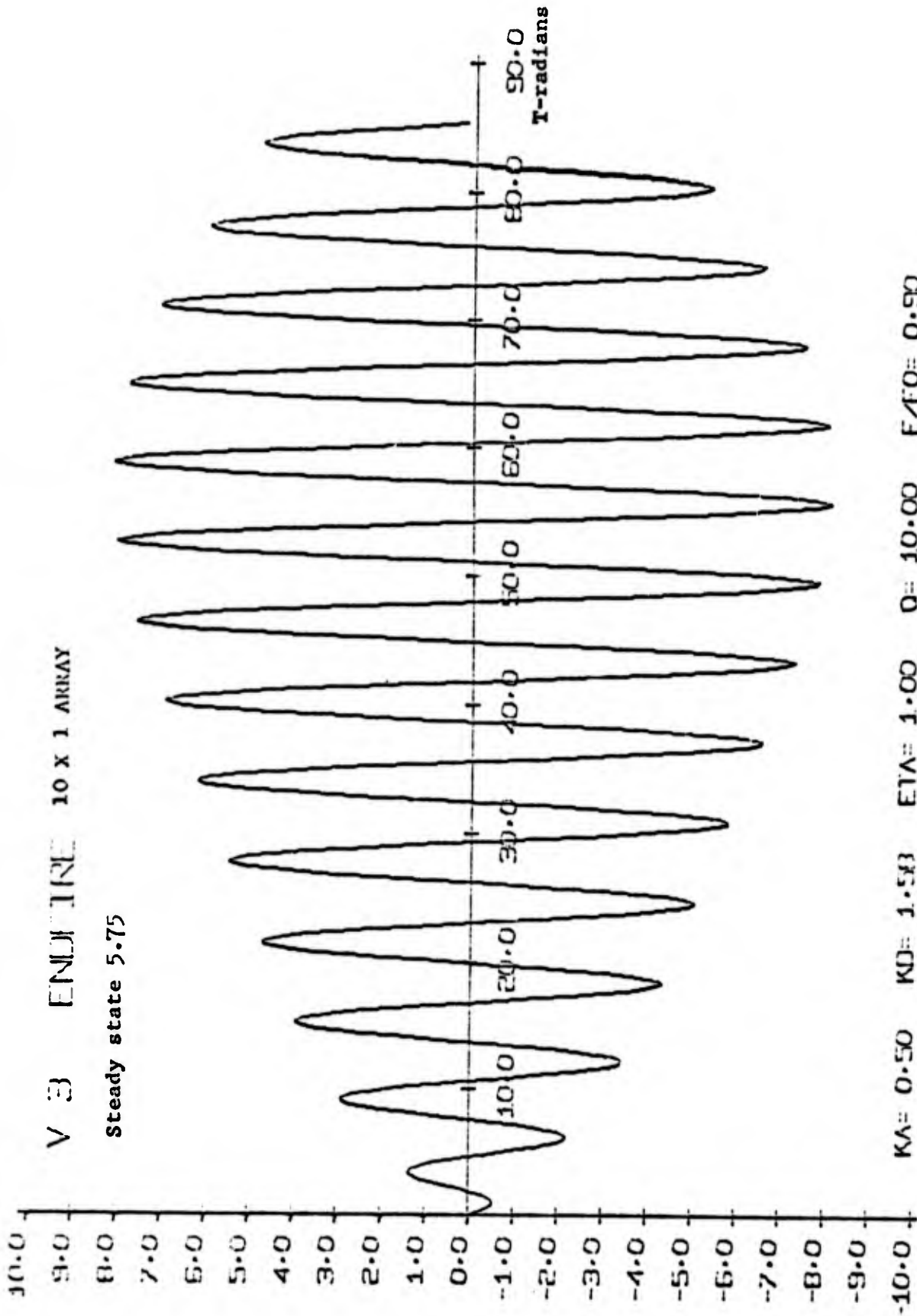


Fig. 12 Velocity of the third transducer in a 10 X 1 line array phased to endfire ( $\beta = 1, \delta = \pi$ ).

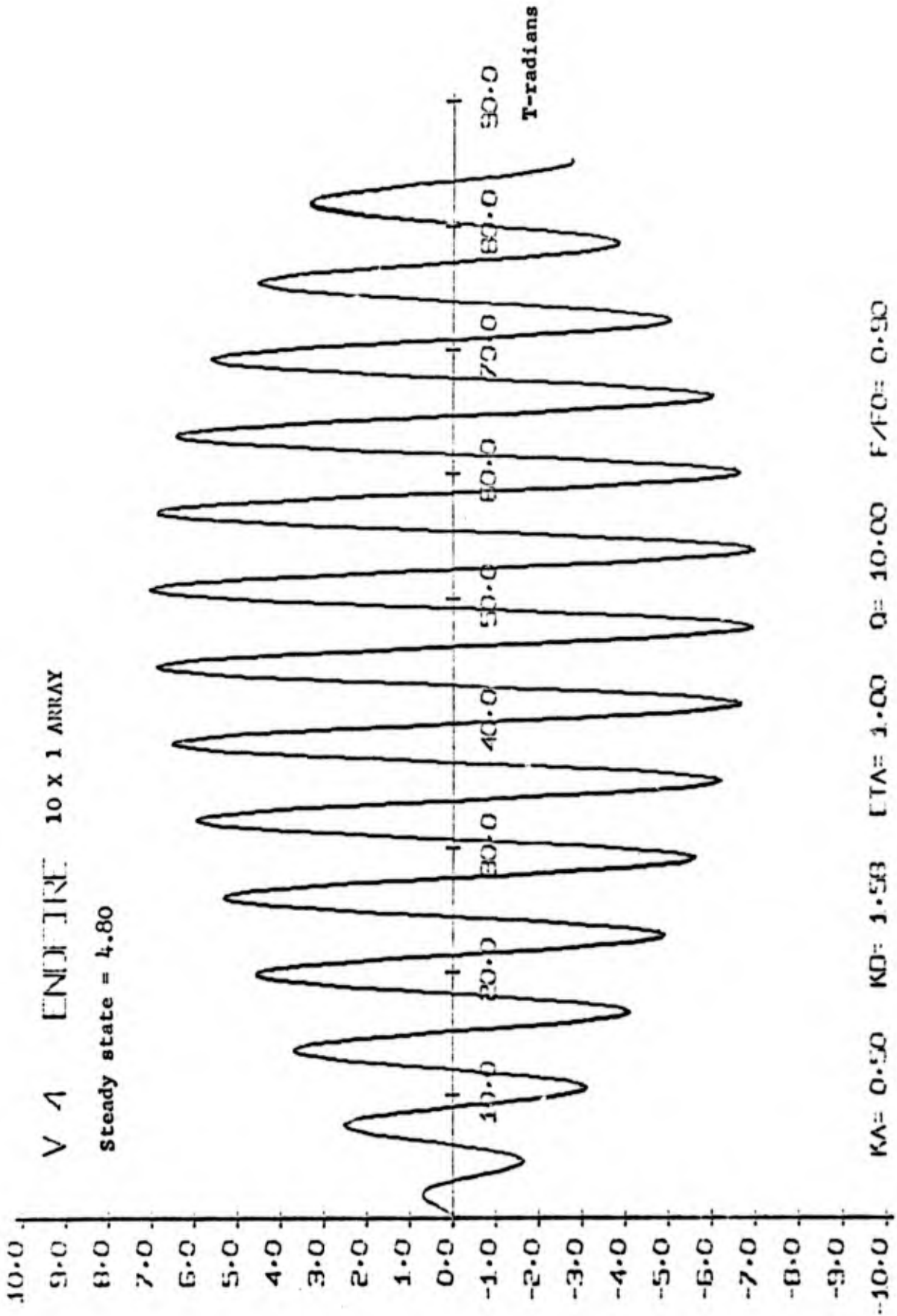


Fig. 13 Velocity of the fourth transducer in a 10 X 1 line array  
 phased to endfire ( $F = 1, \delta = 3\pi/2$ ).

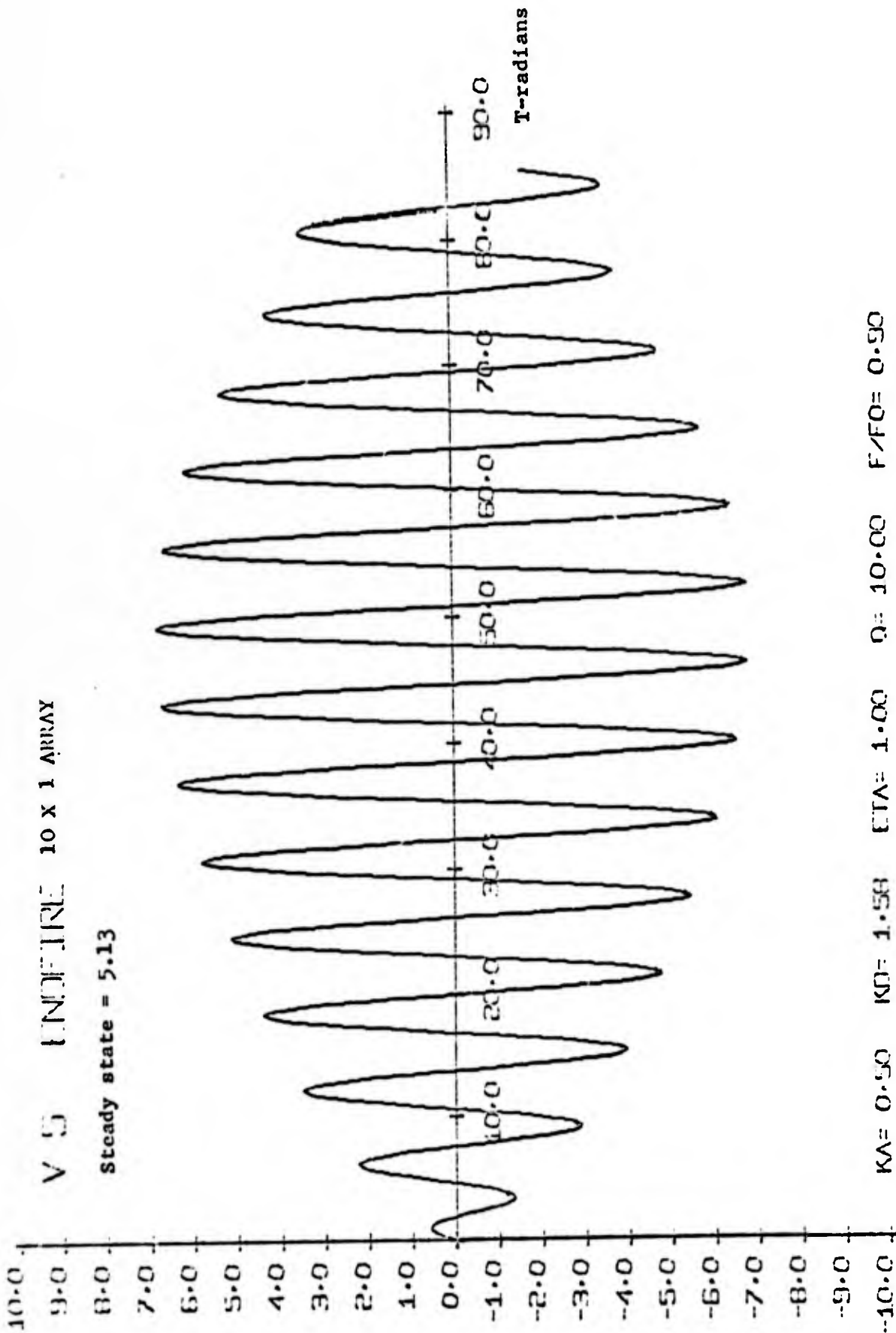


Fig. 14 Velocity of the fifth transducer in a 10 X 1 line array  
 phased to endfire ( $\beta = 1, \delta = 0$ ).

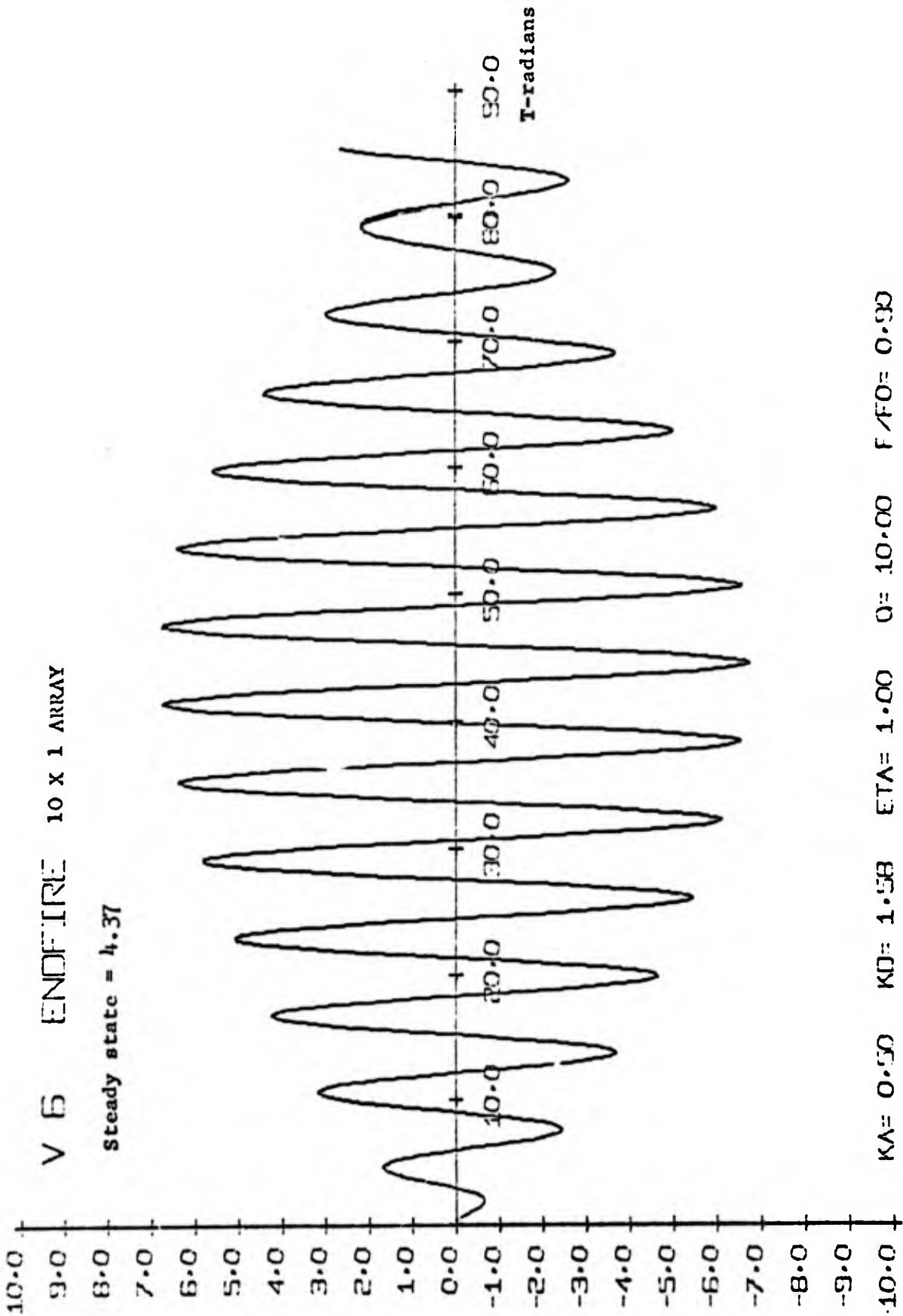


Fig. 15 Velocity of the sixth transducer in a 10 X 1 line array  
 phased to endfire ( $F = 1, \delta = \pi/2$ ).

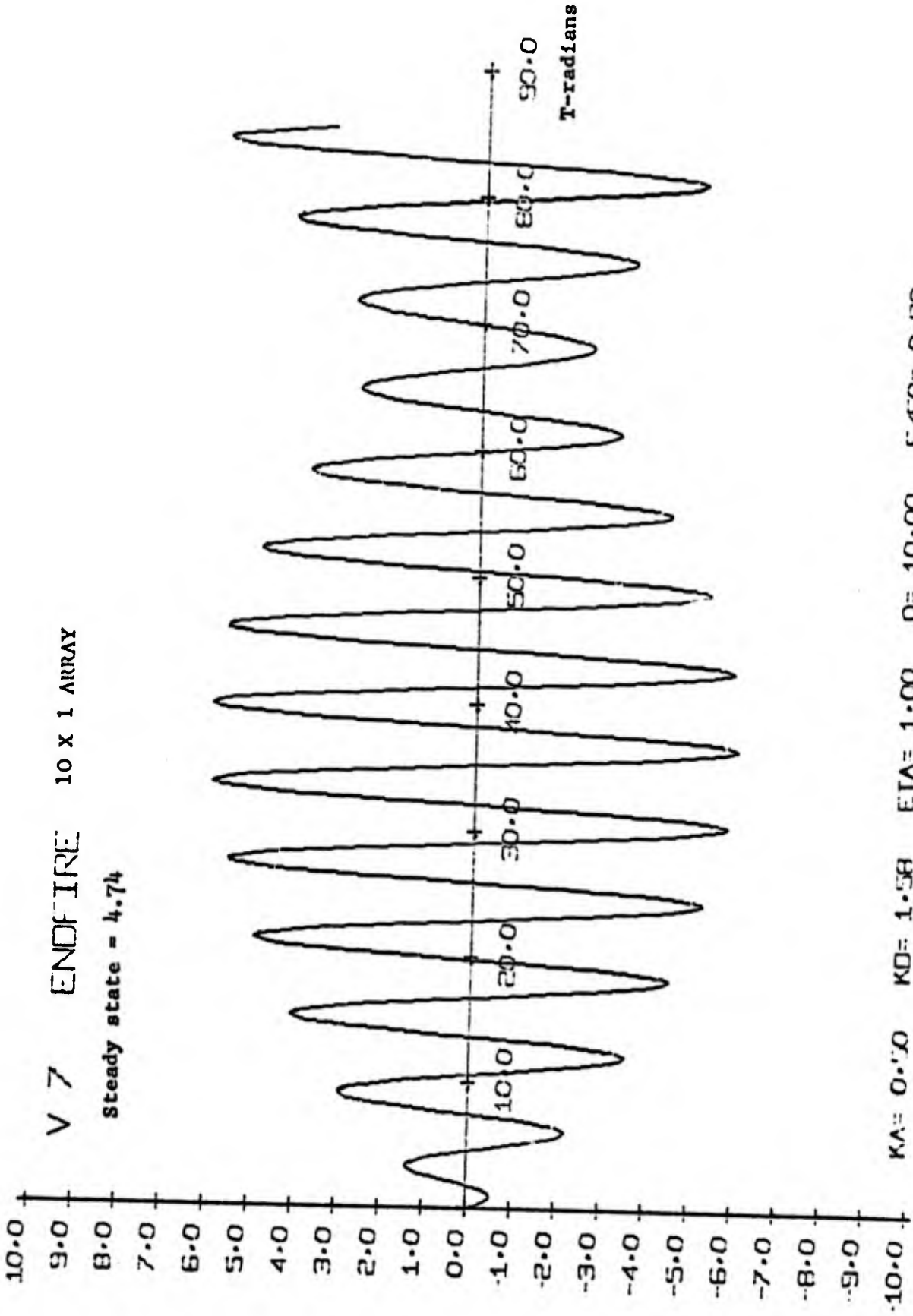


Fig. 16 Velocity of the seventh transducer in a 10 X 1 line array phased to endfire ( $F = 1, \delta = \pi$ ).

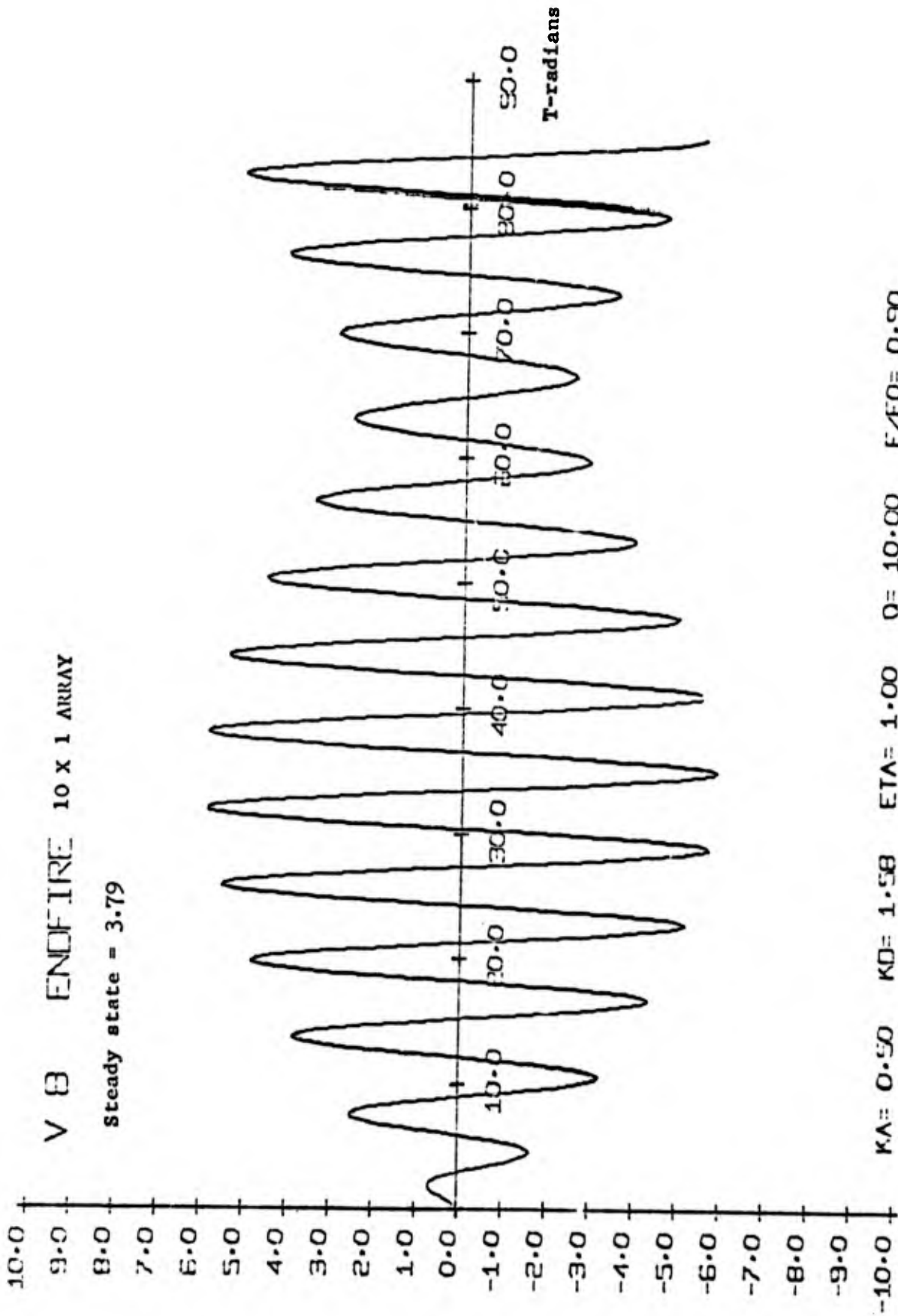


Fig. 17 Velocity of the eighth transducer in a 10 X 1 line array phased to endfire ( $F = 1, \delta = 3\pi/2$ ).

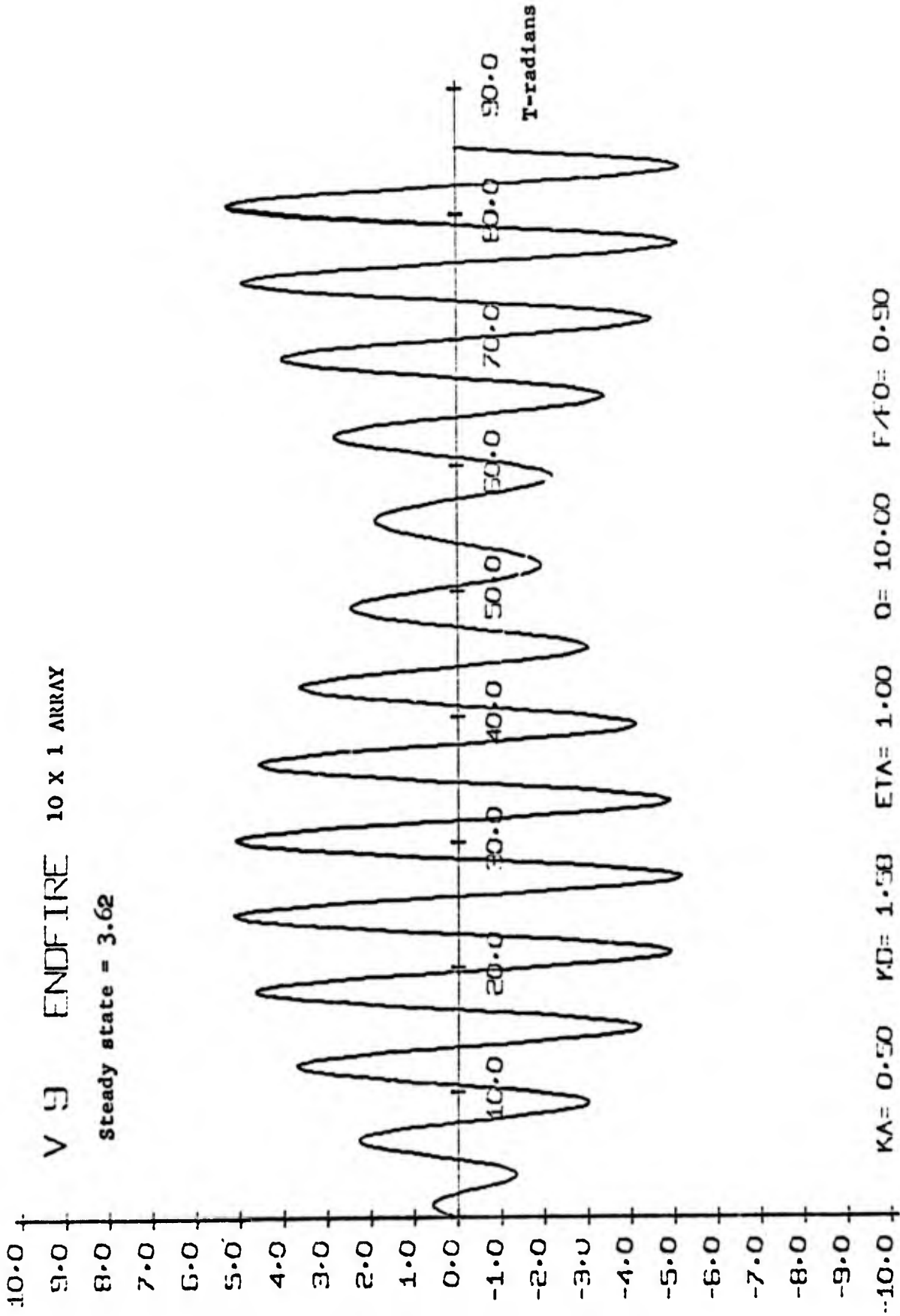


Fig. 18 Velocity of the ninth transducer in a 10 X 1 line array phased to endfire ( $F = 1, \delta = 0$ ).

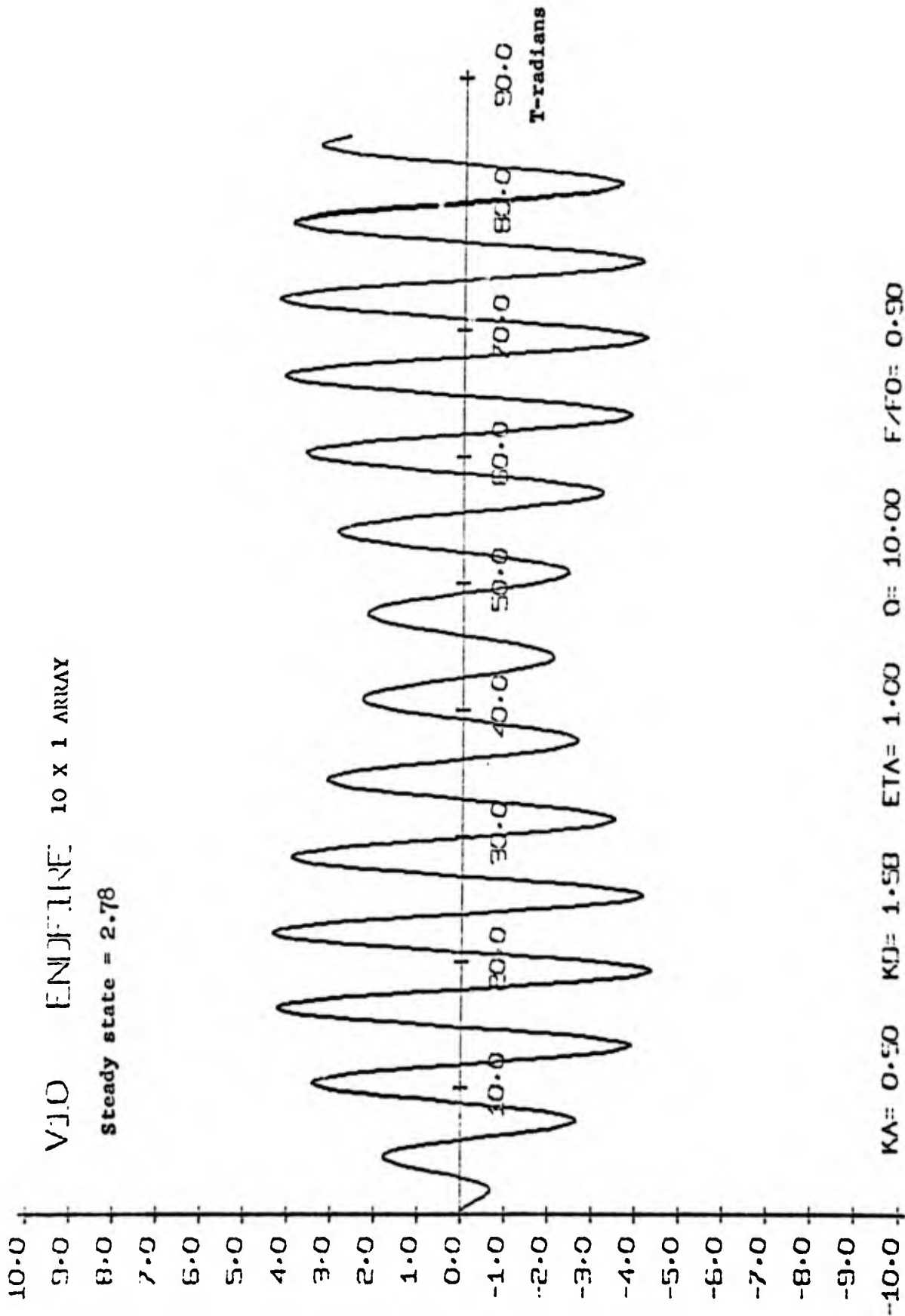


Fig. 19 Velocity of the transducer on the downstream end of a 10 X 1 line array phased to endfire ( $F = 1, \delta = \pi/2$ ).

References

- 1) C.H. Sherman and N.E. Gordon, "Numerical Approach to the Transient Behaviour of Sonar Arrays", PML Tech. Memo. No. 2, Contract No. N00140-66-C-0172, August, 1966.
- 2) J.L. Butler and D.A. Moran, "A Fourier Series Approach to the Transient Solution for Acoustical Arrays", PML Tech. Memo. No. 3, Contract No. N00140-68-C-0109, March, 1968.
- 3) C.H. Sherman and D.A. Moran, "Transient Sound Field of Simple Arrays of Circular Pistons", PML Scientific Report No. 1, Contract No. N00140-66-C-0172, November, 1966.
- 4) Rayleigh, The Theory of Sound Vol.II, Dover, New York, p.107.
- 5) V. Mangulis, Acustica, 17 223 (1966).
- 6) R.L. Pritchard, J. Acoust. Soc. Am. 32 730 (1960).

UNCLASSIFIED

Security Classification

DOCUMENT CONTROL DATA - R&D		
<i>(Security classification of title, body of abstract and indexing annotation must be entered when the overall report is classified)</i>		
1. ORIGINATING ACTIVITY (Corporate author) Parke Mathematical Laboratories, Incorporated One River Road Carlisle, Massachusetts 01741		2a. REPORT SECURITY CLASSIFICATION Unclassified
		2b. GROUP - - -
3. REPORT TITLE TRANSIENT ANALYSIS OF TRANSDUCER ARRAYS		
4. DESCRIPTIVE NOTES (Type of report and inclusive dates) Scientific Interim		
5. AUTHOR(S) (First name, middle initial, last name) Charles H. Sherman Dorothy A. Moran		
6. REPORT DATE May 1968	7a. TOTAL NO. OF PAGES 36	7b. NO. OF REFS 6
8a. CONTRACT OR GRANT NO. N00140-68-C-0109	9a. ORIGINATOR'S REPORT NUMBER(S) Scientific Report No. 1	
b. PROJECT, TASK, WORK UNIT NOS. - - -		
c. DOD ELEMENT - - -	9b. OTHER REPORT NO(S) (Any other numbers that may be assigned this report) - - -	
d. DOD SUBELEMENT - - -		
10. DISTRIBUTION STATEMENT Distribution of this document is unlimited. It may be released to the Clearinghouse, Department of Commerce, for sale to the general public.		
11. SUPPLEMENTARY NOTES - - -	12. SPONSORING MILITARY ACTIVITY U.S. Navy Underwater Sound Laboratory Fort Trumbull New London Connecticut 06301	
13. ABSTRACT A method for analyzing the transient behaviour of the transducer velocities in an array of transducers is described and used to obtain results for several typical situations. The method is based on a finite difference iteration solution of the differential equations for the array. It uses results of Mangulis for the transient self acoustic loading and makes approximations for the acoustic interactions based on Rayleigh's general expression for the field of a source in an infinite, rigid plane. The results obtained are for small plane arrays of small circular pistons. They show that the transient period can be considerably extended by the interactions and that effects of practical importance such as velocity overshoots often occur during the transient period.		

DD FORM 1473  
1 NOV 65

UNCLASSIFIED

Security Classification

**UNCLASSIFIED**

**Security Classification**

14.	KEY WORDS	LINK A		LINK B		LINK C	
		ROLE	WT	ROLE	WT	ROLE	WT
	Transients Transducers Transducer Arrays Underwater Sound						

**UNCLASSIFIED**

**Security Classification**